The Ag-Zr (Silver-Zirconium) System

By I. Karakaya
Middle East Technical University
and
W.T. Thompson
Royal Military College of Canada

Equilibrium Diagram

The equilibrium condensed phases of the Ag-Zr system are: the liquid, L; the Ag-rich fcc (Ag) solid solution; the Zr-rich bcc (βZr) and cph (αZr) solid solutions; and two tetragonal intermediate phases with the approximate compositions AgZr and $AgZr_2$. In addition, [52Kar] claimed the existence of "$AgZr_3$." In the assessed Ag-Zr phase diagram (Fig. 1), the liquid boundary and those for the terminal solutions are based on the thermodynamic computations discussed below. A list of invariant points is given in Table 1. The general appearance of the diagram is similar to that reported by [76Kub].

The Ag-rich solid solution was reported to have very limited Zr solubility, about 0.1 at.% at 900 °C [48Rau, 69Pra]. [48Rau] reported some solubility of Zr in (Ag)—less than 0.1 at.% at 900 °C—based on his being unable to collect supporting evidence for significant solubility by X-ray or micrographic means. [69Pra] performed a series of resistivity, tensile strength, and hardness measurements and concluded that the solubility of Zr in (Ag) increases from about 0.03 at.% at 600 °C to about 0.1 at.% at 900 °C.

Based on thermal and metallographic studies, the constitution in the range 80 to 100 at.% Zr was reported tentatively by [52Kem]. A detailed investigation [58Bet] of Ag-Zr system in the region 64 to 100 at.% Zr by thermal, metallographic, and X-ray analysis showed considerable (20 at.%) Ag solubility in (βZr) at the peritectic temperature (1190 °C). Although the Ag solubility in (αZr) was reported as 1.1 at.% at the eutectoid, this concentration was found to decrease as the level of impurities in Zr increased [58Bet]. The impurities that appear to have the largest effect in reducing the Ag solubility were Fe, C, and Ni [58Bet]. Based upon this effect, the solubility of Ag in (αZr) at the eutectoid (820 °C) is, in the opinion of the authors, very near 1.6 at.%.

The presence of an intermediate phase in the Ag-Zr system was proposed from a microstructural study of alloys with overall compositions up to 33.6 at.% Zr [29Syk]. Subsequently, X-ray analysis [48Rau, 52Kar] confirmed the existence of AgZr. Conflicting results were reported for a second intermediate phase—[52Kar] reported a phase with the approximate composition $AgZr_3$, based on a maximum in X-ray diffraction intensity between compositions 70 to 85 at.% Zr, whereas [52Kem] identified the second Zr-rich intermediate phase as $AgZr_2$, based on metallographical studies in the composition range 58 to 69 at.% Zr. [58Bet] reported a disordered bct structure in the composition range 66 to 67 at.% Zr, from X-ray examinations of slowly cooled specimens. This phase was found to be partially ordered when the specimens were quenched. Subsequently, [62Nev] identified $AgZr_2$ as tetragonal. In this evaluation, the intermediate

Table 1 Special Points of the Assessed Ag-Zr Phase Diagram

Reaction	Compositions of the respective phases, at.% Zr			Temperature, °C	Reaction type
L ↔ Ag		0		961.93	Melting
L ↔ (Ag) + AgZr	2.5	0.1	48.5	940	Eutectic
L + $AgZr_2$ ↔ AgZr	46.5	66.0	50.0	1136	Peritectic
L ↔ (βZr) ↔ $AgZr_2$	63.5	80.2	66.7	1190	Peritectic
(βZr) ↔ (αZr) + ($AgZr_2$)	96.1	97.8	67.0	820	Eutectoid
L ↔ βZr		100		1855	Melting
βZr ↔ αZr		100		863	Allotropic

Table 2 Ag-Zr Crystal Structure Data

Phase	Composition, at.% Zr	Pearson symbol	Space group	Strukturbericht designation	Prototype	Reference
(Ag)	0 to 0.1	*cF*4	$Fm\bar{3}m$	*A*1	Cu	[King1]
AgZr	50	*tP*4	*P*4/*nmm*	*B*11	γCuTi	[Metals]
$AgZr_2$	66.7	*tI*6	*I*4/*mmm*	$C11_b$	$MoSi_2$	[Metals]
(αZr)	100	*hP*2	$P6_3/mmc$	*A*3	Mg	[Metals]
(βZr)	100	*cI*2	$Im\bar{3}m$	*A*2	W	[Metals]

phase "$AgZr_3$" [58Kar] was taken to be an erroneous identification of $AgZr_2$.

Liquidus measurements in the composition range 0 to 50 at.% Zr were reported [48Rau] from thermal analysis. Notably, it is quite flat. The liquidus along the Zr-rich side has apparently not been measured.

Crystal Structures and Lattice Parameters

The crystal structures of Ag-Zr phases are listed in Table 2, and the lattice parameters are given in Table 3. Two lattice parameters are given for AgZr. These are the smallest and the

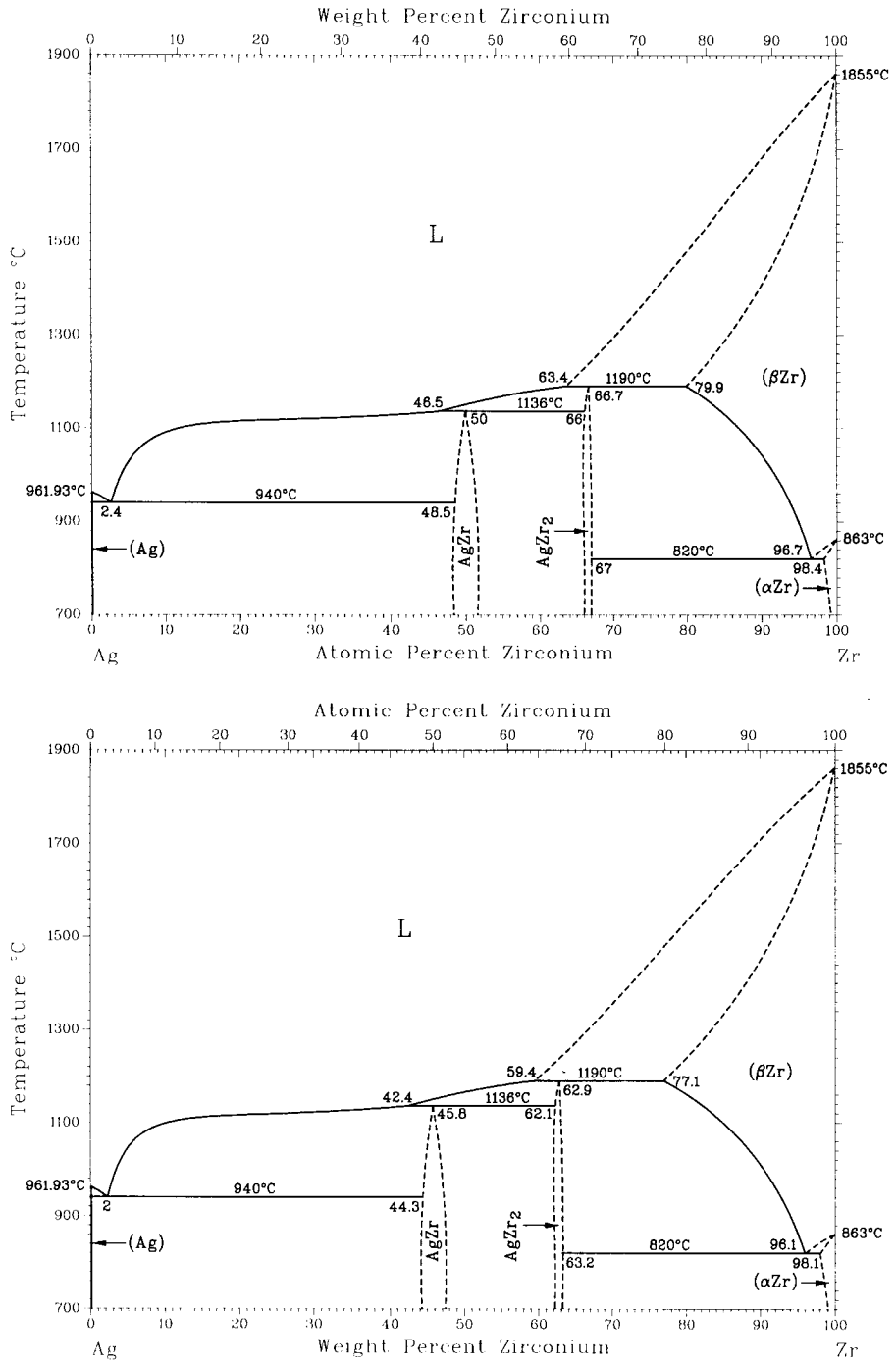

Fig. 1 Assessed Ag-Zr phase diagram. Partially calculated.

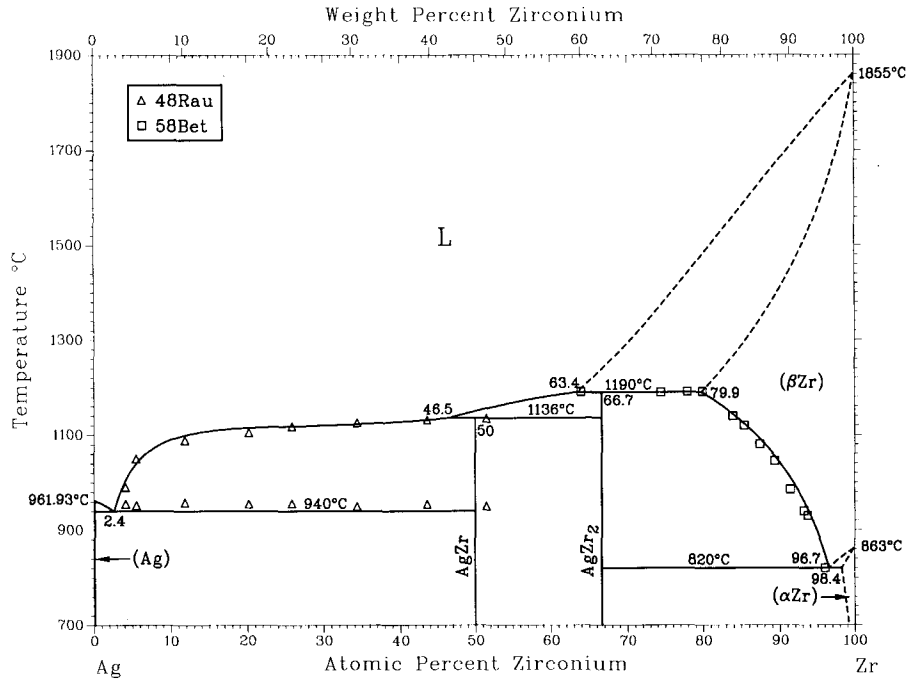

Fig. 2 Calculated Ag-Zr diagram compared with experimental data.

Table 3 Ag-Zr Lattice Parameter Data

Phase	Composition, at.% Zr	Lattice parameters, nm *a*	*c*	Reference
Ag	0	0.40861	...	[King1]
AgZr	50	0.3468	0.6603	[52Kar]
		0.3476	0.6629	[52Kar]
$AgZr_2$	66.7	0.32464	1.20037	[62Nev]
αZr	100	0.32317	0.51476	[King1]
βZr	100	0.3609	...	[King2]

largest values measured [52Kar]. Based on the assumption of Vegard's law, [52Kar] calculated the homogeneity range of AgZr as less than 3 at.%.

Thermodynamics

No thermodynamic properties of any solution phase in the Ag-Zr system were found in the literature. In the present assessment, estimates were used, together with the known thermodynamic properties. Data for pure Ag is consistent with [87Kar]. The transformation entropy for αZr to βZr was taken to be 3.8 J/K g-atom [82Abr]. The specific heat capacity of βZr and liquid Zr as well as the enthalpy of melting were taken from [77Bar]. The Gibbs energy of melting of βZr was adjusted slightly to yield a melting temperature of 1855 °C [83Cha]. Other data shown in Table 4 and listed below as limiting Henrian activity coefficients for terminal solid solutions were introduced to produce the phase diagram shown in Fig. 2.

A subregular-solution model was employed for the liquid phase. Terminal solid phases were considered as Henrian solutions, and the following temperature-independent partial excess Gibbs energies were used for the solutes to obtain reported solubilities. The standard states for Ag and Zr are pure solid Ag and αZr, respectively:

$RT \ln \gamma_{Zr} = 60\,000$ J/mol for the (Ag) phase

$RT \ln \gamma_{Ag} = 17\,400$ J/mol for the (αZr) phase

$RT \ln \gamma_{Ag} = 15\,000 - 4T$ J/mol for the (βZr) phase

Thermodynamic properties for AgZr and $AgZr_2$ formation were calculated to be in accord with the phase diagram. It was sufficient to treat enthalpies and entropies of formation as constants, as shown in Table 4. Small ranges of solubilities for the compounds were not introduced into the modeling.

Table 4 Ag-Zr Thermodynamic Properties

Thermodynamic properties of transformation with respect to the liquid

G^0 (Ag, L) = 0

G^0 (Zr, L) = 0

G^0 (Ag, fcc) = $-1218.86 - 90.7247\,T - 0.4799 \times 10^{-2}\,T^2$
$= 13.74\,T \ln T - 266\,500/T$

G^0 (Zr, cph) = $-14\,000.36 - 65.1432\,T - 0.2322 \pm 10^{-2}\,T^2 + 10.234\,T \ln T$

G^0 (Zr, bcc) = $-9656.96 - 68.9432\,T - 0.2322 \times 10^{-2}\,T^2 + 10.234\,T \ln T$

Estimated thermodynamic properties for the liquid phase

$\Delta H(L) = X_{Ag}X_{Zr}(20\,000 - 37\,000X_{Zr})$

$S^{ex}(L) = 0$

Estimated thermodynamic properties of formation

$\Delta_f G^0$ (Ag, fcc + Zr, cph ↔ AgZr) = $-15\,000 + 2.6\,T$

$\Delta_f G^0$ (Ag, fcc + 2Zr, cph ↔ $AgZr_2$) = $-27\,900 + 6.6\,T$

Note: Values are in J/mol and J/mol· K.

The calculated Ag-Zr phase diagram is compared with the experimental data [48Rau, 58Bet] in Fig. 2.

The calculated diagram is in agreement with the reported solid solubilities of Zr in (Ag) [69Pra] and Ag in (βZr) [58Bet]. The eutectic temperature reported by [48Rau] (955 °C) is higher than that calculated (940 °C) on the basis of Zr solubility and the enthalpy of fusion for Ag. However, a more recent differential thermal analysis study [78Lob] showed the eutectic at 935 °C. Similarly, at the eutectoid (calculated as 820 °C), (βZr) with 3.3 at.% Ag was found in the computation to be in equilibrium with (αZr) with about 1.6 at.% Ag. The conjugate concentrations differ from that reported by [58Bet] (3.9 and 1.1 at.%, respectively). The present evaluation places more emphasis on the extreme sensitivity of Ag solubility to the impurity level in the Zr.

Furthermore, the solubilities of Ag in coexisting αZr and βZr are interrelated by

$$8.314T \ln (1 - X^{\beta}_{Ag})/(1 - X^{\alpha}_{Ag}) = \Delta S^{\alpha \rightarrow \beta}(T - 1136.2)$$

The entropy change is 3.8 J/K g-atom [82Abr]. The present evaluation with respect to Ag solubility in the terminal Zr-rich phases is, in the authors' opinion, the best compromise at the eutectoid temperature.

Both intermetallic compounds apparently melt incongruently. This is in keeping with the reports of [58Bet], [78Lob], and [52Kem]. The possibility of a eutectic between AgZr and $AgZr_2$ suggested by [48Rau] and [58Bet] is not in agreement with the present thermodynamic evaluation.

Suggestions for Future Research

A systematic study of Ag-Zr system is required to resolve uncertainties surrounding the peritectic reactions, the Ag solubility in (αZr), the liquidus near (βZr), and the range of solubility for the intermediate phase AgZr.

Cited References

29Syk: C. Sykes, "Alloys of Zirconium II," *J. Inst. Met., 492*, 179-190 (1929). (Equi Diagram; Experimental)

***48Rau:** E. Raub and M. Engel, "Alloys of Zirconium with Copper, Silver and Gold," *Z. Metallkd., 39*, 172-177 (1948) in German. (Equi Diagram, Thermo; Experimental; #)

52Kar: N. Karlsson, "An X-Ray Study of the Phases in the Silver-Zirconium System," *Acta Chem. Scand., 6*, 1424-1430 (1952). (Equi Diagram, Crys Structure; Experimental)

52Kem: R.S. Kemper, Jr., "The Zirconium-Silver System," M.S. thesis, Oregon State College, Corvallis, OR (1952). (Equi Diagram, Thermo; Experimental; #)

***58Bet:** J.O. Betterton, Jr. and D.S. Easton, "The Silver-Zirconium System," *Trans. Metall. Soc. AIME, 212*, 470-475 (1958). (Equi Diagram, Thermo; Experimental; #)

62Nev: M.V. Nevitt and J.W. Downey, "A Family of Intermediate Phases Having the Si_2Mo-Type Structure," *Trans. Metall. Soc. AIME, 224*, 195-196 (1962). (Equi Diagram, Crys Structure; Experimental)

69Pra: N.L. Pravoverov and Yu.G. Kolonin, "The Solubility of Zirconium in Silver," *Russ. Metall., 2*, 154-155 (1969). (Equi Diagram, Thermo; Experimental; #)

76Kub: O. Kubaschewski and V. Goldbeck, "Phase Diagrams," *Atomic Energy Review, Special Issue, 6* (1976). (Equi Diagram; Compilation; #)

77Bar: I. Barin, O. Knacke, and O. Kubaschewski, *Thermochemical Properties of Inorganic Substances*, Springer-Verlag, Berlin (1977). (Thermo; Compilation)

78Lob: T.P. Loboda, V.N. Pyatnitskii, M.V. Raevskaya, and E.M. Sokolovskaya, "Study of the Zirconium-Silver System by Differential Thermal Analysis," *Vestn. Mosk. Univ. Khim., 19*, 298-301 (1978) in Russian. (Thermo; Experimental)

82Abr: J.P. Abriata and J.C. Bolcich, "The Zr (Zirconium) System," *Bull. Alloy Phase Diagrams, 3*(1), 28 (1982). (Thermo; Compilation)

83Cha: M.W. Chase, "Heats of Transition of the Elements," *Bull. Alloy Phase Diagrams, 4*(1), 124 (1983). (Thermo; Compilation)

87Kar: I. Karakaya and W.T. Thompson, "The Ag-Pb (Silver-Lead) System," *Bull. Alloy Phase Diagrams, 8*(4), 326-334 (1987). (Thermo; Review)

*Indicates key paper.

#Indicates presence of a phase diagram.

Ag-Zr evaluation contributed by **I. Karakaya**, Department of Metallurgical Engineering, Middle East Technical University, Ankara, Turkey, 06351 and **W.T. Thompson**, Department of Chemistry and Chemical Engineering, Royal Military College of Canada, Kingston, Ontario K7K 5L0. This work was supported by a grant from ASM International. Literature searched through 1988. Dr. Thompson is the Alloy Phase Diagram Program Co-Category Editor for binary silver alloys.